J Mater Sci (2007) 42:7630–7637
DOI 10.1007/s10853-007-1900-7

Effect of friction factor on barrelling in elliptical shaped billets during cold upset forging

K. Baskaran · R. Narayanasamy · S. Arunachalam

Received: 12 October 2006 / Accepted: 2 April 2007 / Published online: 16 June 2007

Abstract This work deals with the effect of friction factor of different lubricants on barrelling in elliptical shaped billets during cold upset forging. Experiments were carried out to generate data on cold upset forging of commercially pure aluminium solid of elliptical billets with different lubricants applied on both sides in order to evaluate the effects of friction factor on the forming behavior of barrelling phenomenon under plane stress state condition. The radius of curvature of both major and minor bulge measured conformed to the calculated one using experimental data and the calculations were made with the assumption that the curvature of the bulge followed the form of a circular arc. Three different *b/a* ratios (ratio of minor to major diameter) namely, 0.6, 0.7 and 0.8 and aspect ratio (ratio of height to diameter) of 0.75 were prepared and cold upset forged. The relationship was also established between the various bulge parameters like the hoop strain, the axial strain, the new geometric shape factor, the stress ratio parameters, the major and minor radius of curvature of the bulge and the friction factor 'm' of different lubricants.

Nomenclature

a	Major diameter of the billet
b	Minor diameter of the billet
h_0	Height of the billet
D_0	Major diameter
F	Force
h_f	Height of the billet after deformation
D_B	Bulge diameter of the billet after deformation
D_{TC}	Top contact diameter of the billet after deformation
D_{BC}	Bottom contact diameter of the billet after deformation

K. Baskaran · R. Narayanasamy (✉)
Department of Production Engineering, National Institute of Technology, Tiruchirappalli, Tamilnadu 620 015, India
e-mail: narayan@nitt.edu

S. Arunachalam
School of Computing and Technology, University of East London, London, UK

Introduction

Forging process has become increasingly important in almost all manufacturing industries such as aerospace, steel plants and automobile applications. The upsetting of solid cylinders is an important metal forming process and an important stage in the forging sequence of many products. Since most die forgings commence with an upsetting phase and the deformation in upset forging may cause surface defects at the bulged surface. The deformation characteristics and the mechanical properties of the billet will be influenced not only by the frictional constraints at the die work piece interfaces but also by the geometrical conditions of die and work piece. Thus a thorough understanding of the deformation process (forming behavior) and the factors limiting the forming of sound parts is important not only from a scientific or engineering view point but also from an economic view point.

Friction plays an important role in all metal working processes. In upsetting, the existence of frictional constraints between the dies and the work piece directly affect the plastic deformation of the latter. Frictional effects at the interface between the specimen and the loading surfaces can lead to what is called 'Barrelling' [1] as shown in the Fig. 1b. The presence of friction is a major cause of

concern to all connected with metal forming operations in general and upsetting of cylindrical billets in particular as per literatures and the role of friction in bulk metal forming has been carried out by many researchers [2–5].

Because of the influence of friction at the work piece loading surface interface, the ends of the specimen are restricted from radial expansion. As a consequence, cone shaped zones (shaded regions in the Fig. 1b) [1] of relatively undeformed metal occur at each end of the specimen and, in time, 'Barrelling' becomes pronounced. The stresses and strains under these conditions are no longer uniform. In upsetting the induced stress and strain affected by development of barreling which depends on the friction condition at the die work piece. If the friction is absent at the die work piece interface, the deformation in the cylinder is uniform and the free surface of the cylinder remains straight during the compression. However, the use of lubricants reduces the degree of bulging.

Kulkarni and Kalpakjian [6] assumed that the arc of the barrel is circular or parabolic. Narayanasamy et al. [7] and Bannerjee [8] showed theoretically that the barrel radius could be expressed as a function of height strain and confirmed the same through experimental evidences. For aluminium solid cylinders, Malayappan and Narayanasamy [9] conducted experiments and proved that the bulge diameter of the aluminium solid cylinders decrease with friction factor value and the same has been confirmed for square billets by Manisekar and Narayanasamy [10]. In References [9, 10] only aspect ratio (ratio of height to diameter) has been considered for the evaluation of bulging characteristics using different friction factor of lubricants. Baskaran and Narayanasamy [11] studied the bulging characteristics of preformed irregularly shaped aluminium billets (elliptical billets) during cold upset forging using a lubricant on both sides under different stress state conditions namely the uniaxial, the plane and the triaxial. Sofor no attempt has been made with the elliptical shaped billets under plane stress state condition by considering both *b/a* (ratio of minor to major diameter) and aspect ratios to evaluate the friction factor of different lubricants on barreling phenomenon.

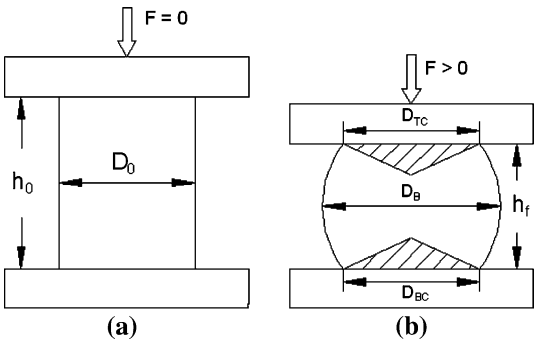

Fig. 1 Experimental set up of cold upsetting of billet (**a**) before deformation; (**b**) after deformation [1]

Experimental details

Cold upsetting specimens of 24 mm in diameter and of different heights corresponding to aspect ratio (initial height to initial diameter ratio) of 0.75 were prepared by machining from 25 mm rods of commercially pure aluminium. These specimens were machined to different ratios of *b/a* (minor diameter/major diameter) namely 0.6, 0.7 and 0.8. The amount of barrelling can be altered by changing the lubrication and height-to-diameter ratio of the specimens as explained by Hosford and Cadell [12]. The cold upsetting of elliptical billets were conducted on a universal compression testing machine having capacity of 100 tons at room temperature with different friction factor value of lubricants as described elsewhere [9] and the same is given in Table 1.

For each test, three specimens were taken and deformed to different strain levels and the detail is shown in Table 2.

The elliptical billets were upset between two flat platens. Extreme care is taken to place the specimens concentric with the axis of the platens. Before cold upsetting the cylinders, the initial diameters such as major diameter ($D_{0\ \text{major}}$), minor diameter ($D_{0\ \text{minor}}$), initial height (h_0) of the specimens and the perimeter before deformation (P_0)

Table 1 Different Friction Factor (*m*) values considered for the tests carried

Lubricant	*m*
Zinc sterrate	0.61
White grease	0.66
Graphite powder + SAE 40	0.69
Dry	0.76

Table 2 Dimension detail of billets used

Major diameter (*a*) (mm)	Minor diameter (*b*) (mm)	h_0 (mm)	*b/a* ratio	h_0/D_0 ratio
24	14.4	18	0.6	0.75
24	16.8	18	0.7	0.75
24	19.2	18	0.8	0.75

a, major axis length; b, minor axis length; h_0, Initial height of billet, D_0, major diameter

were measured. After each incremental loading the following parameters were measured:

1. Major top contact diameter ($D_{TC\ major}$)
2. Minor top contact diameter ($D_{TC\ minor}$)
3. Major bottom contact diameter ($D_{BC\ major}$)
4. Minor bottom contact diameter ($D_{BC\ minor}$)
5. Major bulge diameter ($D_{B\ major}$)
6. Minor bulge diameter ($D_{B\ minor}$)
7. Height after deformation (H_f)
8. Area for top contact surface (A_T)
9. Area for bottom contact surface (A_B)
10. Perimeter for top contact surface (P_T)
11. Perimeter for bottom contact surface (P_B)
12. Major radius of curvature ($R_{m\ major}$) and
13. Minor radius of curvature ($R_{m\ minor}$)

The loads used for each deformation are recorded from the dial indicator of the universal compression-testing machine. Major, minor contact diameters, bulge diameters, height before and after deformations are measured using a digital vernier caliper. Area, perimeter, bulge radius at each lubricated condition is recorded by scanning the elliptical billets using scanner. Further the image is transferred to raster image of Auto CADD where the above said is measured. Figure 2 shows the photograph of undeformed elliptical billet samples of aluminium for various height strains. Figures 3, 4, 5 and 6 shows the photograph of deformed elliptical billet samples of aluminium using dry, zinc sterrate, white grease and graphite powder + SAE 40 lubricants for various height strains.

Fig. 2 Photograph showing billets before deformation

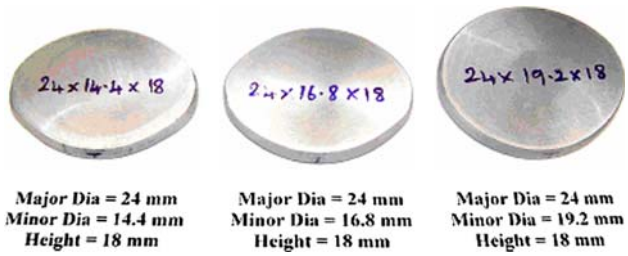

Fig. 3 Photograph showing billets after deformation using dry lubricant

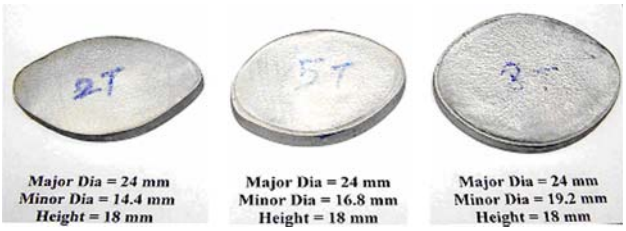

Fig. 4 Photograph showing billets after deformation using zinc-sterrate lubricant

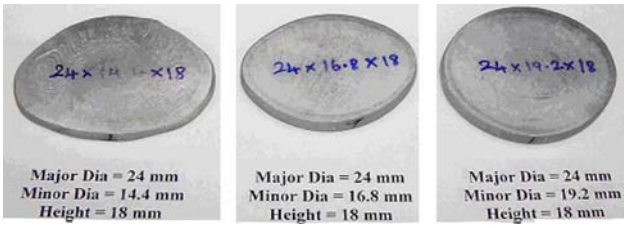

Fig. 5 Photograph showing billets after deformation using white grease lubricant

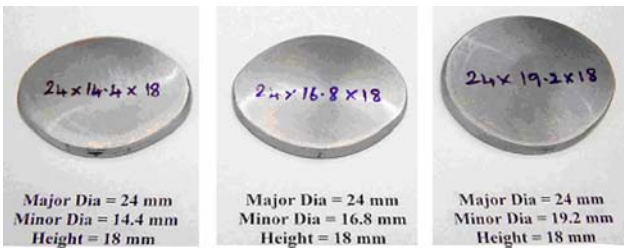

Fig. 6 Photograph showing billets after deformation using graphite + oil lubricant

Theoretical discussion

The mathematical expressions used and proposed for the determination of various upsetting parameters are discussed below:

Radius of the barrel

As explained elsewhere [9], the expression for the circular radius of curvature of barrel is as follows:

$$R = \frac{x}{2} + \frac{{h_f}^2}{8x} \tag{1}$$

Since x is very small, the term $x/2$ can be neglected. Hence, the Eq. 1 becomes

$$R = \frac{{h_f}^2}{4(D_B - D_C)} \tag{2}$$

where D_B is the bulge diameter, D_C is the contact diameter and h_f is the height after deformation.

Derivation of new geometrical shape factor

The volume of metal before deformation is equal to the volume of metal after deformation. This assumption is based on the ''volume constancy principle''.

$$\pi abh_0 = \pi\left(\frac{D_{major}}{2}\right)\left(\frac{D_{minor}}{2}\right)h_f \tag{3}$$

where a is the initial major diameter before deformation, b is the initial minor diameter before deformation, D_{major} is the major diameter of sample after deformation, D_{minor} is the minor diameter of sample after deformation, h_0 is the initial height before deformation, and h_f is the height after deformation.

$$\frac{\pi}{4}(D_{major})(D_{minor}) \times h_0 = h_f \times \frac{\pi}{4}\left[\frac{2(D_{B\,major})(D_{B\,minor}) + (D_{C\,major})(D_{C\,minor})}{3}\right] \tag{4}$$

Simplifying the above Eq. 4, we get

$$\frac{\pi}{4}(D_{major})(D_{minor}) \times h_0 = \frac{\pi}{4}\left[\frac{2(D_{B\,major})(D_{B\,minor}) + (D_{C\,major})(D_{C\,minor})}{3}\right] \times h_f$$

$$\frac{h_0}{h_f} = \left[\frac{2(D_{B\,major})(D_{B\,minor}) + (D_{C\,major})(D_{C\,minor})}{3 \times (D_{major})(D_{minor})}\right] \tag{5}$$

Upon taking natural logarithm on both sides, the Eq. 5 becomes as follows:

$$\ln\left(\frac{h_0}{h_f}\right) = \ln\left[\frac{2(D_{B\,major})(D_{B\,minor}) + (D_{C\,major})(D_{C\,minor})}{3 \times (D_{major})(D_{minor})}\right] \tag{6}$$

In the Eq. 6, the left hand side represents the true axial strain, ε_z and the right hand side shows the expression for the new hoop strain, ε_θ .

From the Eq. 2,

$$R = \frac{{h_f}^2}{4(D_B - D_C)}$$

The above equation can be written as follows for elliptical shaped billets:

$$R_1 = \frac{{h_f}^2}{4(D_{B\,major} - D_{C\,major})} \times \frac{h_0^2}{h_0^2} \tag{7}$$

$$R_2 = \frac{{h_f}^2}{4(D_{B\,minor} - D_{C\,minor})} \times \frac{h_0^2}{h_0^2} \tag{8}$$

From the Eq. 7,

$$R_1 = \left(\frac{{h_f}^2}{h_0^2}\right) \times \frac{h_0^2}{4(D_{B\,major} - D_{C\,major})} \tag{9}$$

Therefore, the Eq. 9 can be written as follows for elliptical shaped billets:

$$R_1 = \left[\frac{3(D_{major})(D_{minor})}{2(D_{B\,major})(D_{B\,minor}) + (D_{C\,major})(D_{C\,minor})}\right]^2 \times \frac{h_0^2}{4(D_{B\,major} - D_{C\,major})} \tag{10}$$

Similarly, the expression for the radius R_2 can be written as follows:

$$R_2 = \left[\frac{3(D_{major})(D_{minor})}{2(D_{B\,major})(D_{B\,minor}) + (D_{C\,major})(D_{C\,minor})}\right]^2 \times \frac{h_0^2}{4(D_{B\,minor} - D_{C\,minor})} \tag{11}$$

where $D_{B\ major}$ is the major bulge diameter, $D_{B\ minor}$ is the minor bulge diameter, $D_{C\ major}$ is the major contact diameter, $D_{C\ minor}$ is the minor contact diameter, D_{major} is the initial major diameter, D_{minor} is the initial minor diameter, h_0 is the initial height of the billets, h_f is the height after deformation, R_1 is the calculated major radius of curvature, and R_2 is the calculated minor radius of curvature.

Uniaxial stress state condition

The mathematical expressions used and proposed for the determination of various upsetting parameters of upsetting for various stress state conditions are discussed below:

The state of stress in a homogeneous compression process is as follows:

According to Abdel-Rahman et al. [13]

$$\sigma_z = -\sigma_{\text{eff}}, \sigma_r = \sigma_\theta = 0 \tag{12}$$

where σ_z is the axial stress, σ_{eff} is the effective stress, σ_r is the radial stress, and σ_θ is the hoop stress.

Since $\sigma_\theta = \sigma_r = 0$ for uniaxial, the hydrostatic stress is given by

$$\sigma_m = \frac{\sigma_z}{3} \tag{13}$$

The axial strain is given by

$$\varepsilon_z = \ln\left[\frac{h_0}{h_f}\right] \tag{14}$$

The hoop stress is given by

$$\varepsilon_\theta = \ln\left[\frac{p_b}{p_0}\right] \tag{15}$$

where ε_z is the axial strain, ε_θ is the hoop strain, P_b is the perimeter after deformation, and P_0 is the perimeter before deformation.

Plane stress state condition

According to Narayanasamy and Pandey [14], the state of stress in a plane stress state condition is as follows:

$$\sigma_{\text{eff}} = (0.5 + \alpha)\left[3\left(1 + \alpha + \alpha^2\right)\right]^{0.5}\sigma_Z \tag{16}$$

where σ_{eff} is the effective stress.

The axial stress is given by

$$\sigma_z = \frac{\text{Load}}{A_C} \tag{17}$$

where σ_z is the axial stress, A_C is the contact area.

Since the $\sigma_r = 0$ at the free surface, it follows from the flow rule that;

$$\sigma_\theta = \left[\frac{1 + 2\alpha}{2 + \alpha}\right] \times \sigma_z \tag{18}$$

where σ_θ is the hoop stress.

The Poisson's ratio is given by

$$\alpha = \frac{\varepsilon_\theta}{\varepsilon_z} \tag{19}$$

where α is the Poisson's ratio. Since the $\sigma_r = 0$ in case of plane stress condition, the hydrostatic stress is given by

$$\sigma_m = \frac{\sigma_\theta + \sigma_z}{3} \tag{20}$$

The effective strain (ε_{eff}) is given by

$$\varepsilon_{\text{eff}} = \left[\frac{2}{3}\left(\varepsilon_z^2 + \varepsilon_\theta^2 + \varepsilon_r^2\right)\right]^{0.5} \tag{21}$$

where ε_z is the axial strain, ε_θ is the hoop strain and ε_r is the radial strain.

Results and discussion

Figure 7 have been drawn between the friction factor (m) and the axial strain (ε_z) for different *b/a* ratios namely, 0.6, 0.7 and 0.8, for the aspect ratio (h_0/D_0) of 0.75 and for the load of 210 KN. The inference from the graph is that a straight line relationship is established between the two parameters irrespective of the *b/a* and the aspect ratios. The behavior is due to increase of axial strain values with respect to the friction factor (m) value and as the *b/a* ratio increases, the axial strain value also increase with the friction factor value.

Figure 8 show the relationship between the friction factor (m) and the hoop strain (ε_θ) for different *b/a* ratios namely, 0.6, 0.7 and 0.8, for the aspect ratio (h_0/D_0) of 0.75 and for the load of 210 KN. The graph establishes a straight line relationship between the two parameters namely, the friction factor (m) and the hoop strain (ε_θ) irrespective of the *b/a* ratios.

Figures 9 and 10 drawn between the measured bulge radius (R_m) and the calculated bulge radius (R_c) for both major and minor radius, for different *b/a* ratios namely, 0.6, 0.7 and 0.8 and for the aspect ratio (h_0/D_0) of 0.75 based on the principle of volume constancy during plastic deformation, and the assumption that the barrel radius follows the circular arc. The calculated values of the radius of curvature of the barrel are in close proximity with the measured values, i.e. a straight line relationship. Hence, the assumption that the bulge barrel radius follows circular arc

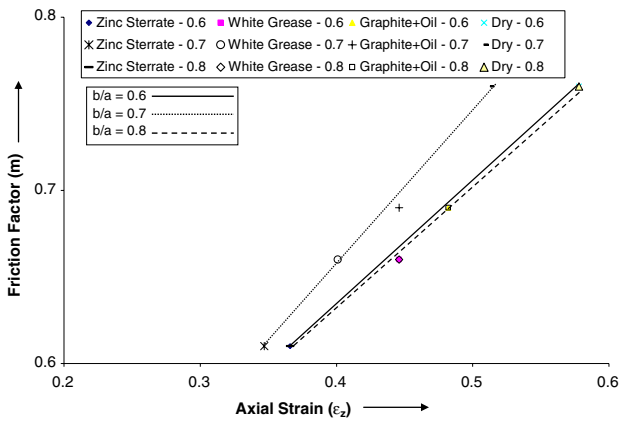

Fig. 7 Friction factor (m) versus axial strain (ε_z) for *b/a* = 0.6, 0.7 and 0.8, $h_0/D_0 = 0.75$ and Load 210 KN

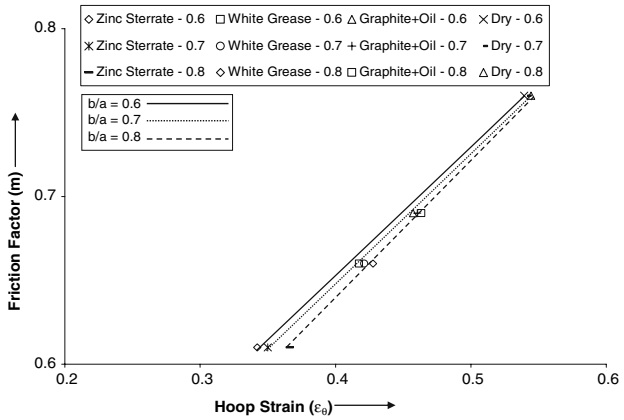

Fig. 8 Friction factor (m) versus hoop strain (ε_θ) for b/a = 0.6, 0.7 and 0.8, $h_0/D_0 = 0.75$ and Load 210 KN

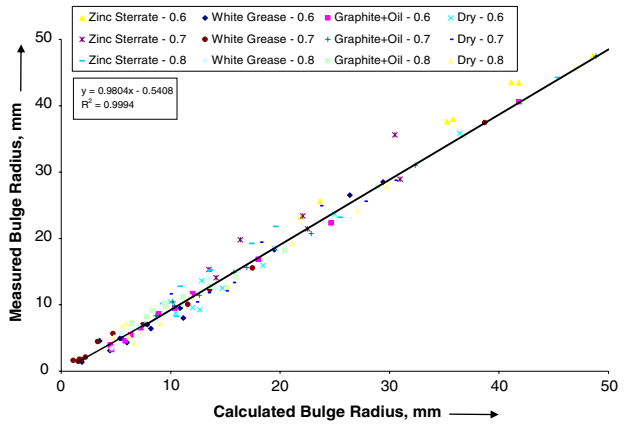

Fig. 9 Measured bulge radius (R_m), major versus calculated bulge radius (R_c), major for b/a = 0.6, 0.7 and 0.8, $h_0/D_0 = 0.75$

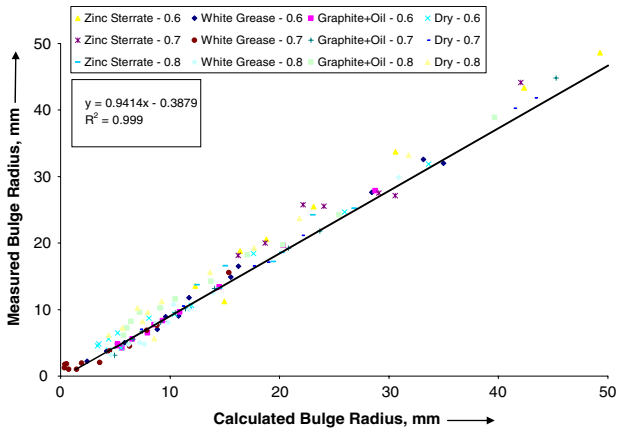

Fig. 10 Measured bulge radius (R_m), minor versus calculated bulge radius (R_c), minor for b/a = 0.6, 0.7 and 0.8, $h_0/D_0 = 0.75$

is correct. When upsetting elliptical shaped billets two types of barrel radius namely barrel radius ($R_{m\ major}$) along major axis and barrel radius ($R_{m\ minor}$) along minor axis, have been observed by the investigators. In both cases, the measured radius of curvature of the barrel is in close proximity with the calculated values with the slope of 1.0 irrespective of the b/a ratios investigated.

Figures 11 and 12 show the relationship between the friction factor (m) and the natural logarithm of calculated radius (R_c) for both major and minor radius, for different b/a ratios namely, 0.6, 0.7 and 0.8, for the aspect ratio (h_0/D_0) of 0.75 and for the load of 300 KN. The bulge radius is observed to decrease linearly with the friction factor values and the slope observed is different for different b/a ratios and is tabulated in Table 3. Further a steep decrease in bulge radius is observed for higher b/a ratio compared to lower b/a ratio, because of less work hardening.

Figures 13 and 14 plot the friction factor (m) against the natural logarithm of NGSF for two different axes of elliptical shaped billets namely major and minor, for different b/a ratios namely, 0.6, 0.7 and 0.8, for the aspect

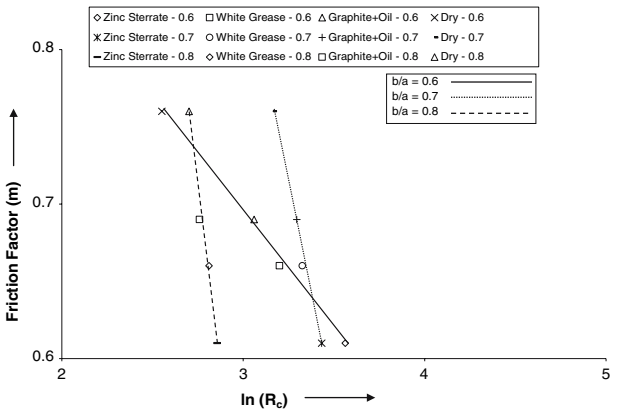

Fig. 11 Friction factor (m) versus natural logarithm of calculated radius (R_c), major for b/a = 0.6, 0.7 and 0.8, $h_0/D_0 = 0.75$ and Load 300 KN

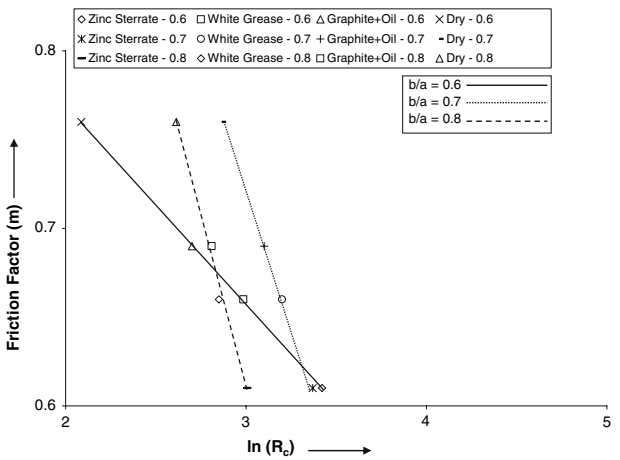

Fig. 12 Friction factor (m) versus natural logarithm of calculated radius (R_c), minor for b/a = 0.6, 0.7 and 0.8, $h_0/D_0 = 0.75$ and Load 300 KN

Table 3 Slope value for different parameters

S. No.	Parameter	*b/a* ratio	Slope
1.	Friction factor versus axial strain	0.6	3.219
		0.7	2.314
		0.8	1.852
2.	Friction factor versus hoop strain	0.6	2.003
		0.7	2.101
		0.8	2.321
3.	Friction factor versus natural logarithm of calculated radius (major)	0.6	0.355
		0.7	1.317
		0.8	1.946
4.	Friction factor versus natural logarithm of calculated radius (minor)	0.6	0.269
		0.7	0.520
		0.8	0.909
5.	Friction factor versus natural logarithm of NGSF (major)	0.6	0.211
		0.7	0.418
		0.8	0.180
6.	Friction factor versus natural logarithm of NGSF (minor)	0.6	0.410
		0.7	0.484
		0.8	0.294
7.	Friction factor versus natural logarithm of SRP (major)	0.6	0.689
		0.7	2.802
		0.8	1.890
8.	Measured radius versus calculated radius (major)	0.6	1.009
		0.7	0.971
		0.8	0.960
9.	Measured radius versus calculated radius (minor)	0.6	0.967
		0.7	0.941
		0.8	0.947

ratio (h_0/D_0) of 0.75 and for the load of 200 KN. These Figures exhibit straight line relationship showing that the geometrical shape factor decreases linearly with the friction factor irrespective of *b/a* for minor radius and reverse is the case for major radius. The slope of the above straight line is found to be different for different *b/a* ratios tested and is shown in Table 3. The rate of change of the friction factor (m) with respect to the natural logarithm of NGSF is not same for different *b/a* ratios tested. This means that the barreling depends on friction and other factors namely, *b/a* and aspect ratios. This proves that the radius of curvature of barrel follows the circular arc during plastic deformation of the elliptical shaped billets. Further it is also observed that the slope of straight line is different for major axis radius and minor axis radius.

Figure 15 is the relationship between the friction factor (m) and the natural logarithm of stress ratio parameter $(\ln[(\sigma_m/\sigma_{eff})(h_0 - h_f)10^2])$ for different *b/a* ratios namely, 0.6, 0.7 and 0.8, for the aspect ratio (h_0/D_0) of 0.75 and for the load of 300 KN. The plot shows the straight-line

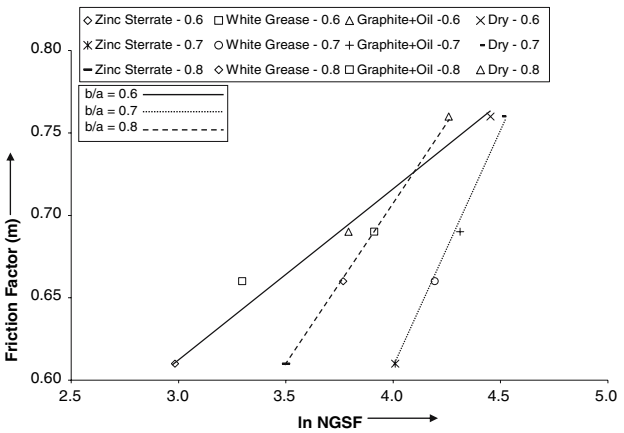

Fig. 13 Friction factor (m) versus natural logarithm of NGSF, major for *b/a* = 0.6, 0.7 and 0.8, $h_0/D_0 = 0.75$ and Load 200 KN

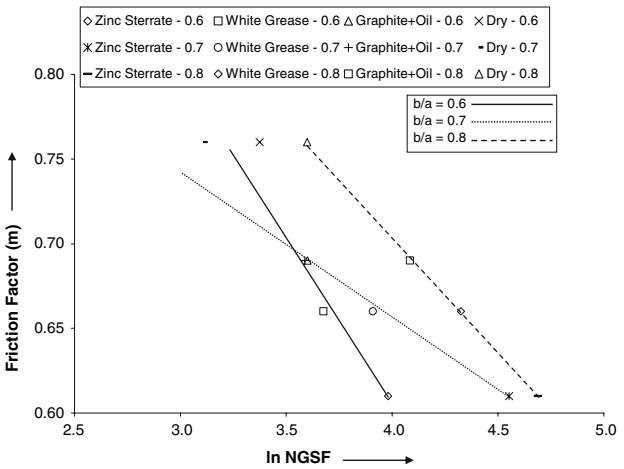

Fig. 14 Friction factor (m) versus natural logarithm of NGSF, minor for *b/a* = 0.6, 0.7 and 0.8, $h_0/D_0 = 0.75$ and Load 200 KN

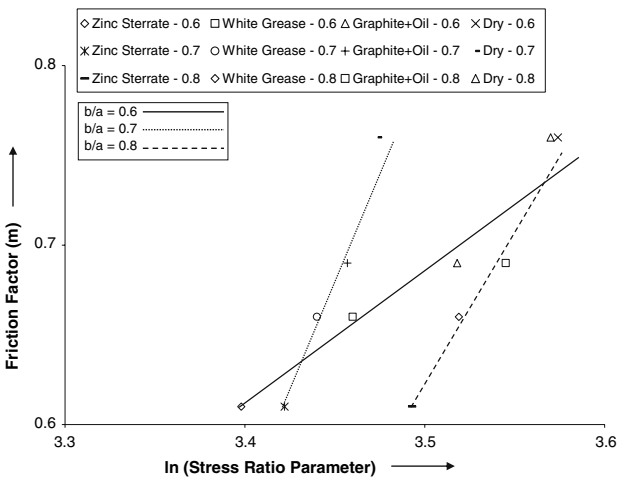

Fig. 15 Friction factor (m) versus natural logarithm of stress ratio parameter $(\ln[(\sigma_m/\sigma_{eff})(h_0 - h_f)10^2])$ for *b/a* = 0.6, 0.7 and 0.8, $h_0/D_0 = 0.75$ and Load 300 KN

relationship between the two parameters namely, the friction factor (m) and the natural logarithm of stress ratio parameter $(\ln[(\sigma_m/\sigma_{eff})(h_0 - h_f)10^2])$.

Conclusion

The following conclusions can be drawn from the present investigation:

1. Among the four lubricants tested namely, zinc sterrate, white grease, graphite powder + SAE 40 and dry lubricant, the most efficient lubricant was zinc sterrate, with a friction factor of 0.61, lower than all the others.
2. The bulge diameter of the elliptical billets decrease with friction factor value. Hence, the bulge diameter produced is lowest for zinc sterrate and highest for dry lubrication at any given strain level, irrespective of *b/a* and aspect ratios tested.
3. The calculated and the measured radii of curvature (major and minor) of barrel are in close proximity.
4. It was found that the barrel radius follows a power law relationship with the new geometrical shape factor and the stress ratio parameter, viz.

   (a) $R = CS^{-m}$

   (b) $R = C_1\left[\left(\frac{\sigma_m}{\sigma_{eff}}\right)(h_0 - h_f)\right]^{-m_1}$

   where R is the radius of curvature, S is the new geometrical shape factor, σ_m is the hydrostatic or mean stress, σ_{eff} is the effective stress, h_0 is the initial height of the sample billets, h_f is the height after deformation, and C, m, C_1 and m_1 are the experimentally determined values.
5. The rate of change of the friction factor (m) with respect to the natural logarithm of NGSF is not same for different *b/a* ratios tested. This means that the barreling depends on friction and other factors namely, *b/a* and aspect ratios.

References

1. Hosford WF, Cadell RM (1993) Metal forming mechanics and metallurgy. Prentice Hall, USA, p 62 (Chapter 3)
2. Johnson W, Mellor PB (1975) Engineering plasticity. Van Nostrand Reinhold, London, pp 110–114 (Chapter 6)
3. Manisekar K, Narayanasamy R (2004) J Trans Indian Inst Met 57(2):141
4. Abdul A (1981) Ann CIRP 30:143
5. Yang DY, Choi Y, Kim JH (2004) Int J Mech Tools Manufact 44(4)
6. Kulkarni KM, Kalpakjian S (1969) ASME J Eng Ind 91:743
7. Narayanasamy R, Murthy RSN, Viswanatham K, Chary GR (1988) J Mech Working Technol 16:21
8. Banerjee JK (1985) ASME J Eng Mater Technol 107:138
9. Malayappan S, Narayanasamy R (2003) Mater Sci Technol 19:1705
10. Manisekar K, Narayanasamy R (2006) Mater Design 27:147
11. Baskaran K, Narayanasamy R (2007) Mater Design, in press
12. Hosford WF, Cadell RM (1983) Metal forming mechanics and metallurgy. Prentice Hall, USA, p 247 (Chapter 11)
13. Abdel-Rahman M, El-Sheikh MN (1995) J Mater Process Technol 54:97
14. Narayanasamy R, Pandey KS (1997) J Mater Process Technol 70:17